COVID-19 progression in hospitalized patients using follow-up *in vivo* CT and *ex vivo* microCT

Vincent Geudens[1]^, Jan Van Slambrouck[1]^, Gitte Aerts[1], Lynn Willems[1]^, Tinne Goos[1]^, Janne Kaes[1]^, Andrea Zajacova[2]^, Iwein Gyselinck[1]^, Celine Aelbrecht[1], Astrid Vermaut[1]^, Hanne Beeckmans[1], Marie Vermant[1]^, Charlotte De Fays[3], Annelore Sacreas[1]^, Lucia Aversa[1], Michaela Orlitova[4]^, Arno Vanstapel[1]^, Ivan Josipovic[5], Matthieu N. Boone[5]^, John E. McDonough[6]^, Birgit Weynand[7]^, Charles Pilette[3], Wim Janssens[1]^, Lieven Dupont[1], Wim A. Wuyts[1]^, Geert M. Verleden[1]^, Dirk E. Van Raemdonck[1]^, Robin Vos[1], Ghislaine Gayan-Ramirez[1]^, Laurens J. Ceulemans[1]^*, Bart M. Vanaudenaerde[1]^*

[1]Laboratory of Respiratory Diseases and Thoracic Surgery, BREATHE, Department of Chrometa, KU Leuven, Leuven, Belgium; [2]Prague Lung Transplant Program, Department of Pneumology, Motol University Hospital, 2nd Faculty of Medicine, Charles University in Prague, Prague, Czech Republic; [3]Department of Pneumology, Cliniques Universitaires Saint-Luc, Institute of Experimental and Clinical Research, Université Catholique de Louvain, Brussels, Belgium; [4]Division of Anesthesiology and Algology, Department of Cardiovascular Sciences, KU Leuven, Leuven, Belgium; [5]Department of Physics and Astronomy, Centre for X-Ray Tomography (UGCT), Radiation Physics, Ghent University, Gent, Belgium; [6]Section of Pulmonary, Critical Care, and Sleep Medicine, Yale University School of Medicine, New Haven, CT, USA; [7]Department of Imaging & Pathology, KU Leuven, Leuven, Belgium

Contributions: (I) Conception and design: V Geudens, BM Vanaudenaerde, LJ Ceulemans, J Van Slambrouck, G Gayan-Ramirez, G Aerts; (II) Administrative support: V Geudens, BM Vanaudenaerde, LJ Ceulemans, J Van Slambrouck, G Gayan-Ramirez; (III) Provision of study materials or patients: V Geudens, BM Vanaudenaerde, LJ Ceulemans, J Van Slambrouck, G Aerts, J Kaes, L Willems, T Goos, I Gyselinck, C Aelbrecht, A Vermaut, H Beeckmans, M Vermant, C De Fays, A Sacreas, L Aversa, M Orlitova, A Vanstapel, A Zajacova, JE McDonough, C Pilette, W Janssens, L Dupont, WA Wuyts, GM Verleden, DE Van Raemdonck, R Vos; (IV) Collection and assembly of data: V Geudens, G Aerts, T Goos, J Van Slambrouck, B Weynand, BM Vanaudenaerde, JE McDonough, I Josipovic, MN Boone; (V) Data analysis and interpretation: V Geudens, G Aerts, L Willems, T Goos, B Weynand, BM Vanaudenaerde, LJ Ceulemans; (VI) Manuscript writing: All authors; (VII) Final approval of manuscript: All authors.

*These authors contributed equally to this work and should be considered as last senior authors.

Correspondence to: Vincent Geudens, MSc. Laboratory of Respiratory Diseases and Thoracic Surgery, BREATHE, Department of Chrometa, KU Leuven, Herestraat 49, Leuven 3000, Belgium. Email: vincent.geudens@kuleuven.be.

Background: Severe acute respiratory syndrome coronavirus 2 (SARS-CoV-2) causes coronavirus disease-19 (COVID-19) which can lead to acute respiratory distress syndrome (ARDS) and evolve to pulmonary fibrosis. Computed tomography (CT) is used to study disease progression and describe radiological patterns in COVID-19 patients. This study aimed to assess disease progression regarding lung volume and density over time on follow-up *in vivo* chest CT and give a unique look at parenchymal and morphological airway changes in "end-stage" COVID-19 lungs using *ex vivo* microCT.

Methods: Volumes and densities of the lung/lobes of three COVID-19 patients were assessed using follow-up *in vivo* CT and *ex vivo* whole lung microCT scans. Airways were quantified by airway segmentations on whole lung microCT and small-partition microCT. As controls, three discarded healthy donor lungs were

^ ORCID: Vincent Geudens, 0000-0002-4386-1746; Jan Van Slambrouck, 0000-0002-7069-1535; Lynn Willems, 0000-0002-1260-7083; Tinne Goos, 0000-0002-8081-333X; Janne Kaes, 0000-0002-3326-3769; Andrea Zajacova, 0000-0002-9691-2500; Iwein Gyselinck, 0000-0002-4068-7228; Astrid Vermaut, 0000-0002-4145-491X; Marie Vermant, 0000-0001-8546-8638; Annelore Sacreas, 0000-0003-1448-3704; Michaela Orlitova, 0000-0002-5295-9315; Arno Vanstapel, 0000-0003-2412-8001; Matthieu N. Boone, 0000-0002-5478-4141; John E. McDonough, 0000-0003-2497-0258; Birgit Weynand, 0000-0003-4246-6303; Wim Janssens, 0000-0003-1830-2982; Wim A. Wuyts, 0000-0001-9648-3497; Geert M. Verleden, 0000-0003-3048-2429; Dirk E. Van Raemdonck, 0000-0003-1261-0992; Ghislaine Gayan-Ramirez, 0000-0001-9652-7437; Laurens J. Ceulemans, 0000-0002-4261-7100; Bart M. Vanaudenaerde, 0000-0001-6435-6901.

used. Histology was performed in differently affected regions in the COVID-19 lungs.

Results: *In vivo*, COVID-19 lung volumes decreased while density increased over time, mainly in lower lobes as previously shown. *Ex vivo* COVID-19 lung volumes decreased by 60% and all lobes were smaller compared to controls. Airways were more visible on *ex vivo* microCT in COVID-19, probably due to fibrosis and increased airway diameter. In addition, small-partition microCT showed more deformation of (small) airway morphology and fibrotic organization in severely affected regions with heterogeneous distributions within the same lung which was confirmed by histology.

Conclusions: COVID-19-ARDS and subsequent pulmonary fibrosis alters lung architecture and airway morphology which is described using *in vivo* CT, *ex vivo* microCT, and histology.

Keywords: Airway morphology; coronavirus disease-19 (COVID-19); *ex vivo* micro-computed tomography (*ex vivo* microCT); *in vivo* chest CT; lung density and volume

Introduction

The severe acute respiratory syndrome coronavirus 2 (SARS-CoV-2) pandemic has brought many challenges into the field of medicine. As of 7 February 2023, over 754 million people have been infected worldwide, causing over 6.8 million deaths due to coronavirus disease-19 (COVID-19) as reported by the World Health Organization (1). Despite being the third known coronavirus inflicting a massive immunological response, affecting mainly lungs (following SARS-CoV-1 and middle east respiratory syndrome-

coronavirus epidemics), the mechanism underlying the lung pathology caused by SARS-CoV-2 infection remains unknown. COVID-19 is characterized by an inter-individual variability in severity of the disease course. In the majority of patients, it is self-resolving, with a clinical course ranging from none to mild symptoms (2). Nevertheless, there is a subgroup of patients with a severe disease course and strong inflammatory response leading to development of acute respiratory distress syndrome (ARDS), resulting in high mortality (3). COVID-19-ARDS is the result of viral pneumonia causing diffuse inflammatory lung injury characterized by disruption of the alveolar-capillary membrane with edema, loss of aerated lung tissue and impaired gas exchange (4,5). In some patients surviving severe or even mild disease, long COVID-19 is seen in which lung abnormalities remain present months after hospital discharge as consequence of COVID-19 infection. Long COVID-19 can result in symptoms like chest pain, breathlessness, muscle weakness, cognition problems, anxiety, and depression (6,7) indicating the importance of understanding the mechanisms and progression of COVID-19 in patients (8). Early in the pandemic, chest computed tomography (CT) became a useful method to diagnose COVID-19 (9,10). Currently, chest CT is necessary for the characterization of lung damage, as it remains irreplaceable to monitor and evaluate disease course in patients with persistent and severe COVID-19 (11). Different severity levels of COVID-19 are characterised by diverse CT changes (12,13) and radiological patterns have been described by the Radiological Society of North

---

Highlight box

Key findings
- Large and small airway morphology is rapidly and severely altered in COVID-19 patients.

What is known and what is new?
- COVID-19 causes rapid lung damage as seen on CT follow-up scans.
- Altered large airway morphology with traction bronchiectasis is present in COVID-19 lungs.
- Using a cascade of state-of-the-art CT techniques (*in vivo* CT, whole lung microCT and small-partition microCT), this study detailed the deleterious impact of COVID-19 on lung architecture with destroyed parenchyma and alteration of large and small airway morphology and similarities seen in IPF lungs.

What is the implication, and what should change now?
- Patients can be monitored using volume and density measures on CT to follow disease progression. Small airway disease should not be neglected in the progression of COVID-19 disease.

America introducing typical CT patterns of COVID-19 (14,15). These include multifocal ground glass opacities (GGO) with or without consolidations, with a bilateral and peripheral distribution, septal and pleural thickening, crazy paving, and traction bronchiectasis (16,17). Less observed indeterminate or atypical appearances are isolated lobar and diffuse GGO, "tree-in-bud", vascular enlargement, halo signs and cavitations (18). As already shown, traction bronchiectasis and fibrosis are present in COVID-19 which might cause homeostatic disruption of the conducting airway system (19). Volume and density measurements have also been performed on *in vivo* chest CT and revealed that lung volumes and density decreased and increased, respectively in COVID-19 patients especially in the lower lobes (20,21). This highlights the possibility to measure these parameters using follow-up *in vivo* chest CT scans to assess disease progression. Hence, there is an urgent need to understand the changes in lung structures and airways in COVID-19 patients, however, a comprehensive analysis and description of radiological parenchymatous and especially (small) airway changes are lacking, and this will be addressed in the present study. Therefore, we determined how COVID-19 affects the lung *in vivo* (volume, density) and *ex vivo* (volume, lung density, radiological patterns, and airway disruption) in severely affected patients, by a combination of follow-up *in vivo* chest CT and *ex vivo* microCT imaging. MicroCT has the advantage that it has a substantial superior resolution granting us the possibility to be able to describe the radiological changes in a very detailed way. *In vivo* and *ex vivo* CT scans were also compared to non-COVID-19 ARDS and idiopathic pulmonary fibrosis (IPF) on the level of to assess differences in disease. We present this article in accordance with the STROBE reporting checklist (available at https://jtd.amegroups.com/article/view/10.21037/jtd-22-1488/rc).

Methods

Study design

Right human lungs from three patients were obtained at the University Hospital Leuven, between January and June 2022, with a positive polymerase chain reaction (PCR) test for SARS-CoV-2 prior to hospitalization. The sample size was three as no other patients were transplanted for consequences after COVID-19 infection. Two COVID-19 lungs were obtained at lung transplantation (COVID-1 and 2), and one was retrieved from an autopsy (COVID-3) of a

patient who received a double lung transplantation for α1-antitrypsin deficiency 8 years prior to infection. COVID-19 lungs were compared to three donor lungs discarded for bacterial meningitis, suspected edema and pneumonia in the opposite lung, respectively which served as control lungs. COVID-3 had an *in vivo* CT scan before COVID-19 infection which was used to compare lung volume after COVID-19 infection. Donor lungs were matched for gender and lung side (right). To compare COVID-19 to non-COVID-19-ARDS and IPF, explanted lungs from patients who underwent lung transplantation for ARDS (n=1, transplantation after 60 days of initial pneumonia) and IPF (n=1) were used. C-reactive protein (CRP) was measured in serum/plasma with a maximum of 5 days between measurements, except for COVID-1 in whom data were missing between day 14 and 56 due to the transfer of hospitals. For IPF, the last value before transplantation was shown. The study was conducted in accordance with the Declaration of Helsinki (as revised in 2013). The collection of lungs and the morphological analysis and imaging study was approved by the Ethical Committee of UZ/KU Leuven (Nos. S51577 and S52174) and written informed consent was obtained from patients for the use of samples for research. Discarded donor lungs were collected in accordance with Belgian law stating that all qualified donors of which organs are not of sufficient quality or remain unused for other reasons can be used for research.

Disease progression in COVID-19 patients was followed over time by analyzing all available non-contrast *in vivo* CT scans. Clinical *in vivo* CT scans (n=4 for COVID-1, n=5 for COVID-2, and n=3 for COVID-3) were acquired using a Siemens Somatom (settings 100–120 kV, 48–562 mA, B-reconstruction kernel, 0.625–3 mm slice thickness) and analysed to measure volume and attenuation [Hounsfield units (HU)]. Whole lung *ex vivo* multidetector CT (MDCT) and microCT were performed on frozen expanded explant lungs to measure lung/lobe volumes, and for airway segmentation in order to assess airway number and diameter.

Volume, density, and airway analysis

In vivo follow-up CT-scans were used for clinical evaluation to monitor COVID-19 ARDS disease progression using a COVID-19 CT protocol (0.6–3 mm slice thickness), to measure volume and density over time. In addition, volume and attenuation were also assessed *in vivo* in one non-implanted control lung (control 1), one COVID-19 patient

Table 1 Performed CT scans in subjects

Subjects	*In vivo* non-COVID	*In vivo* COVID	*Ex vivo* microCT	*Ex vivo* MDCT
COVID-1		x	x	
COVID-2		x	x	
COVID-3	x	x	x	
Control 1	x		x	
Control 2			x	
Control 3			x	
ARDS	x			x
IPF	x			x

"x" means performed CT scans in subjects. CT, computed tomography; COVID, coronavirus disease; MDCT, multidetector CT; ARDS, acute respiratory distress syndrome; IPF, idiopathic pulmonary fibrosis.

prior to COVID-19 infection, one ARDS and one IPF lung to compare volumes and density of whole lungs and lung lobes (*Table 1*). Volumes were calculated automatically or manually (when the lung could not be discriminated from the surrounding tissue due to increased density) using Mimics Innovation Suite 24 (Materialise, Leuven, Belgium; RRID:SCR_012153). Whole-lung microCT was performed on frozen lungs of controls and COVID-19 patients to assess volume and airway characteristics using a custom microCT protocol in collaboration with Ghent University (22), (resolution ±155 µm). The IPF and ARDS lung were scanned using *ex vivo* MDCT (Siemens Somatom, 120 kV, 110 mA, reconstruction kernel 1.0 b60f, 1 mm slice thickness). Volumes of lung/lobes were calculated by manually lining lobes in 3D Slicer (RRID:SCR_005619). No HU could be reported of the whole lung microCT but microCT image density was calibrated by taking two datapoints of known density to develop a linear scale across tissue density values. Airspace density (0 g/mL) was used to determine background density levels and the density of the insertion tube (0.775 g/mL) was used as second datapoint for linear regression. Tissue density was then calculated along this scale. HU and g/mL can be converted by (HU + 1,000)/1,000 = g/mL (23). Airways of control and COVID-19 lungs were automatically segmented using Mimics Innovation Suite 24 (Materialise; RRID:SCR_012153). IPF and ARDS were not segmented as whole lung microCT scans were not available. Airways which were not connected to the main airway tree and two first generations were excluded for analysis. Airway number and average inner diameter per generation were assessed using NeuronStudio (RRID:SCR_013798). Small airways were visualized using small-partition microCT on lung cores. Lung cores were imaged using a Skyscan 1172 microCT scanner (Bruker, Kontich, Belgium) with a resolution of 9.9 µm and small airways were segmented by segmentation using ITK-SNAP (RRID:SCR_002010) (24).

Lung collection

Whole right lungs were collected following a protocol adapted from McDonough *et al.* (25). After explantation, lungs were cannulated into the primary or secondary bronchus, inflated to total lung capacity using compressed air, frozen in vapors of liquid nitrogen and stored at –80 ℃. Total lung volume, density, and airway characteristics were obtained by *ex vivo* MDCT and whole-lung microCT. The frozen lungs were sliced in the axial plane with a bandsaw into 2 cm slices. Subsequently, samples (cores) of regions of interest, based on evaluation of the scan and macroscopic pictures, were taken with an electrical power drill (1.4 cm) to assess the whole spectrum of small airway morphology and deformations present in the lung.

Histological analysis

Samples (n=3/lung, 1 mild, 1 moderate, and 1 severe) used for small-partition microCT were stained with hematoxylin and eosin (H&E) to visualize airway and alveolar structure and with Masson's trichrome to detect collagen deposition leading to fibrosis. Sections (5 µm) of lung cores, fixed in

Table 2 Patient characteristics

Parameters	COVID-1	COVID-2	COVID-3	Control 1	Control 2	Control 3	IPF	ARDS
Gender	Male	Male	Male	Male	Male	Male	Male	Female
Race	Caucasian	Caucasian	Caucasian	Caucasian	Caucasian	Caucasian	Caucasion	Caucasian
Age (years)	39	46	64	56	24	68	59	26
Height (m)	1.78	1.80	1.72	1.69	1.70	1.76	1.74	1.56
Weight (kg)	80	80	72	76	53	76	82	65
BMI (kg/m^2)	25	25	24	27	18	25	27	27
Smoking	Stopped	No	Stopped pre-SSLTx	No	No	No	Yes	No
Pack years	23	NA	10	NA	NA	NA	10	NA
Relevant medical history	–	–	COPD (AATD) SSLTx 2013 (no CLAD)	Bacterial meningitis	Pneumonia, DBD	Pneumonia left lung, DCD	–	Overwhelming pneumonia
COVID-19 vaccination	No	No	1st dose BNT162b2, 4 days before onset COVID-19	No	No	No	No	No
Chronic medication	None	None	Standard triple IS	NA	NA	NA	NA	NA
Infection ICU	Bacterial, aspergillosis	Bacterial	Bacterial	NA	NA	NA	NA	NA

COVID, coronavirus disease; IPF, idiopathic pulmonary fibrosis; ARDS, acute respiratory distress syndrome; BMI, body mass index; SSLTx, sequential-single lung transplantation; NA, not applicable; COPD, chronic obstructive pulmonary disease; AATD, alpha-1 antitrypsin deficiency; CLAD, chronic lung allograft dysfunction; DBD, donor after brain death; DCD, donor after cardiac arrest; IS, immunosuppression; ICU, intensive care unit.

4% paraformaldehyde overnight at 4 ℃ and processed into paraffin, were stained with H&E after rehydration. For Masson's trichrome staining, sections were rehydrated, fixed in Bouin's solution overnight before staining with Weigert's iron hematoxylin, Biebrich Scarlet-acid fuchsin, and aniline blue. Slides were digitalized using a digital pathology slide scanner (Philips IntelliSite Ultra-Fast Scanner, Best, The Netherlands). Sections were analyzed by a trained pathologist (BW).

Statistical analysis

Ex vivo volumes of control and COVID-19 lungs were reported as mean ± standard deviation (SD) and compared with a Student's *t*-test after normality testing using a Shapiro-Wilk test. The ARDS and IPF lung were excluded from the analysis.

Results

Patient characteristics

Patient characteristics are presented in *Table 2* and timeline of events are available in Table S1. Patients were transplanted or deceased 65.3±26.7 days after onset of symptoms. Time course measures of CRP show an initial state of inflammation (COVID-19-ARDS), with increased CRP values above standard levels of <5 mg/mL especially in COVID-2. CRP levels decrease transiently to increase again in all COVID patients when the fibrotic phase started just before the need for transplantation or death (Figure S1).

In vivo and ex vivo volume analysis

Four, five and three *in vivo* chest CT scans were performed in COVID-1, COVID-2, and COVID-3 patients, respectively (Table S1). Total lung volume decreased over time in COVID-2 and 3 patients, with the largest decrease in the first 20 days. By contrast, total lung volume in COVID-1 declined gradually probably due to a delayed first scan (day 14). Compared to control 1 and COVID-3 before infection, volume decreased from 6.10±0.25 to 2.29±0.18 L in COVID-19 patients. This was related to a decrease in left and right lung volume. Missing values of lobe volumes in COVID-1 and 2 were due to the inability to distinguish separate lobes. Lobar volumes decreased compared to control 1 and COVID-3 prior to infection. *In vivo* and *ex vivo* volumes were comparable for the COVID-19 lungs indicating the relevance of studying the *ex vivo* lung alterations. *Ex vivo* volumes of whole right lungs in COVID-19 patients were decreased compared to control (4.22±0.26 *vs.* 1.55±0.49 L, P<0.0037) as seen in *in vivo* scans. This was caused by a significant decrease in upper (1.47±0.26 *vs.* 0.59±0.08 L, P<0.019), middle (0.63±0.10 *vs.* 0.26±0.13 L, P<0.018) and lower (2.12±0.10 *vs.* 0.71±0.45 L, P<0.027) lobe volume. *In vivo* and *ex vivo* volumes of the IPF and ARDS lung were equivalent compared to COVID-19 volumes (*Figure 1*).

Ex vivo airway morphology changes

MicroCT scans showed decreased volumes (*Figure 1*) and altered airway morphology in COVID-19 lungs compared to controls was seen visually (*Figure 2*, *Video 1*). Segmentations demonstrated a heterogeneity of airway damage between but also within COVID-19 lungs. In more proximal generations (up to ±10), the visible number of airways was higher in control lungs, however, the visible number of small airways (<2 mm) was lower while the visible number of large airways was higher compared to COVID-19 patients, indicating distortion of smaller airways (*Figure 3A*). In more distal generations, there were more large and small airways in COVID-19 indicating an increase in visibility due to bronchiectasis and increased attenuation around small airways. The prevalence of large airways (>2 mm) increased from generation 15 in controls to generation 22 in COVID-19 lungs. There were no differences in mean airway diameter per generation (*Figure 3B*) between control and COVID-19. To correct for the increase in visible small airways in COVID-19,

airway numbers in each generation were equalized to the data of the lung with the lowest number of airways in that generation to normalize for the higher number of visible airways in COVID-19 (*Figure 3C*). After normalization, the diameter of lower generations (17-21) was higher in COVID-19.

In vivo and ex vivo density assessment

In vivo density of left and right lungs gradually increased in all COVID-19 lungs (*Figure 4A*). Four days after onset of symptoms, density increased compared to control 1 and COVID-3 before infection. *Ex vivo* densities (expressed in g/L) of COVID-19 right lungs were comparable with *in vivo* densities (expressed in HU) of the last scan, showing the resemblance between *in vivo* and *ex vivo* scans, and were higher compared to *ex vivo* densities of ARDS and IPF (*Figure 4A*). In the right and left lungs (*Figure 4B,4C*), density of the lower lobe increased more than in other lobes similarly to IPF.

Radiological features

Typical, indeterminate, and atypical radiologic features, as determined by the Radiological Society of North America (14), were present in all COVID-19 lungs. However, variable patterns were seen in each COVID-19 lung (*Figure 5*). COVID-1 was characterized by homogeneous distribution of GGO with diffuse consolidations and traction bronchiectasis in all lobes especially in the lower lobe and subpleural honeycomb-like changes in all lobes. COVID-2 has a patchy distribution of GGO with crazy paving, consolidations mainly present in the lower lobe and subpleural parenchyma of the upper lobe. Parenchyma of the middle lobe was less severely affected compared to the upper and lower lobe. Traction bronchiectasis was more prominent in the lower lobe. A reticular pattern, resulting from thickening of interlobular and intralobular septa was seen in the upper and middle lobe. COVID-3 was characterized by a heterogeneous distribution of GGO with consolidations, diffuse traction bronchiectasis in all lobes and cyst formation. In the upper lobe, GGO were more present on the posterior side, whereas consolidations were more prominent on the anterior side, while the opposite was observed in the lower lobe. In all COVID-19 lungs, airways were often disconnected from the main tree by obstructions with mucus or fibrosis. These are also characteristics which are
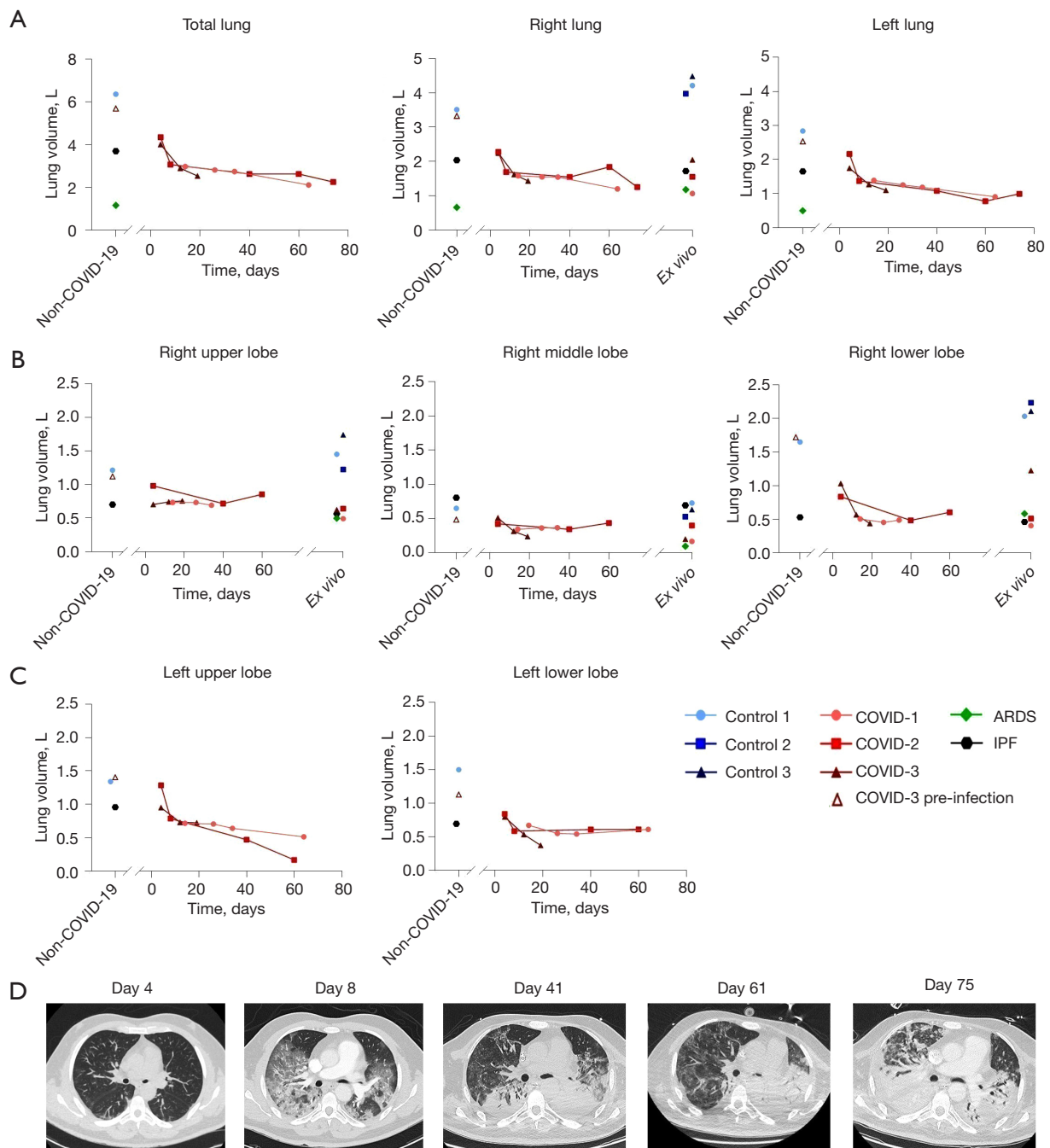
Figure 1 *In vivo* and *ex vivo* volumes of the non-COVID-19 and COVID-19 lungs and lobes. (A) *In vivo* volumes in lungs without COVID-19 namely one control, COVID-3 before infection, ARDS, and IPF (non-COVID-19) and lungs with COVID-19 (red) showing a gradual decrease over time in COVID-19 patients. *Ex vivo* volumes of explant lungs are depicted for the right lung showing a significant decrease (P<0.0058) in right lung volume in COVID-19 lungs compared to controls. (B) Volumes of the right lung lobes are shown *in vivo* and *ex vivo*. The *ex vivo* volumes significantly decreased in the upper (P<0.018), middle (P<0.022), and lower lobe (P<0.024). (C) *In vivo* volumes gradually decrease in the left upper and middle lobe. Missing values were due to unrecognizable fissures/lobes. (D) Follow-up *in vivo* scans of COVID-2 showing the decline in lung volume. COVID-19, coronavirus disease-19; ARDS, acute respiratory distress syndrome; IPF, idiopathic pulmonary fibrosis.
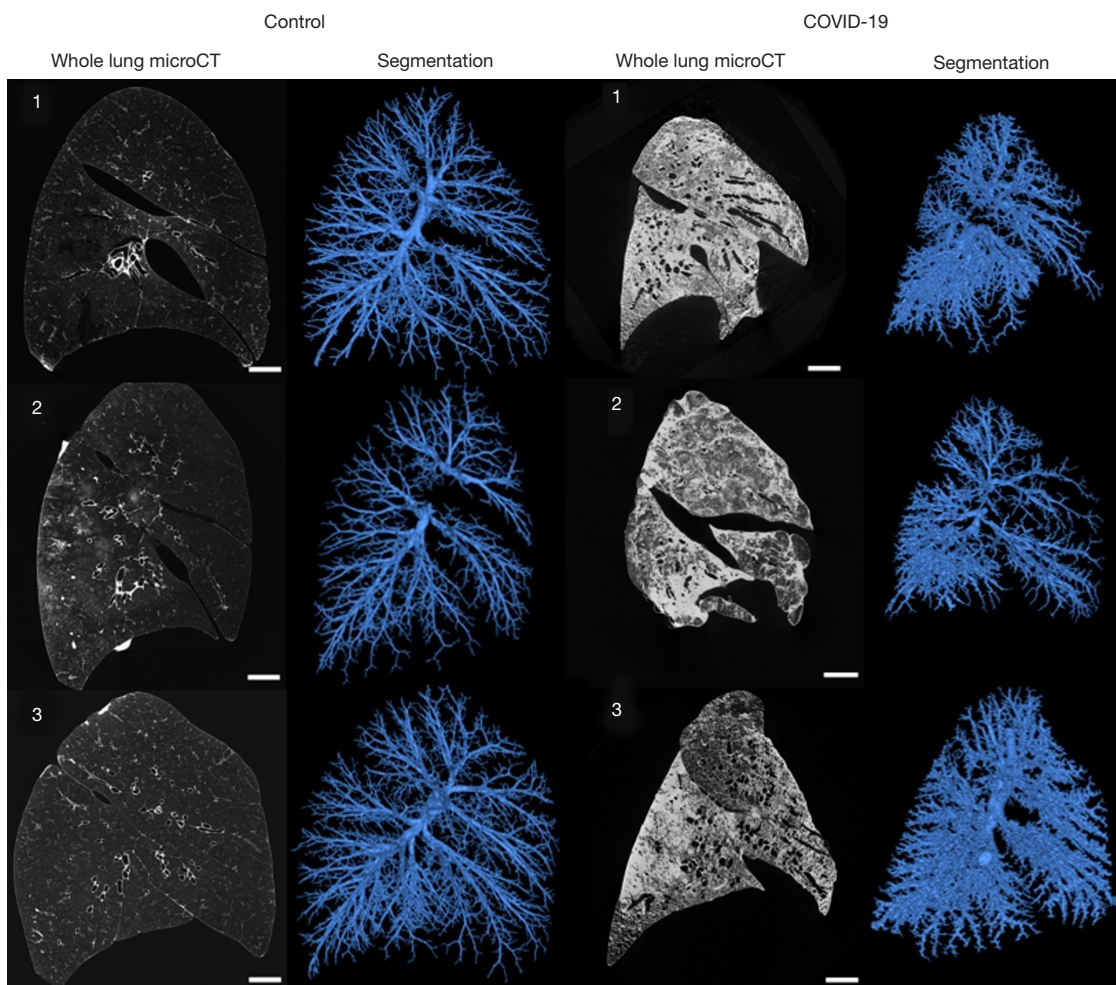
Figure 2 Airway segmentations with the corresponding microCT scan. Whole lung microCT scans of control (left) and COVID-19 (right) lungs are shown from control/COVID-19 1 (top) to 3 (bottom) with its corresponding airway segmentation. Scale bar =3 cm. COVID-19, coronavirus disease-19; CT, computed tomography.
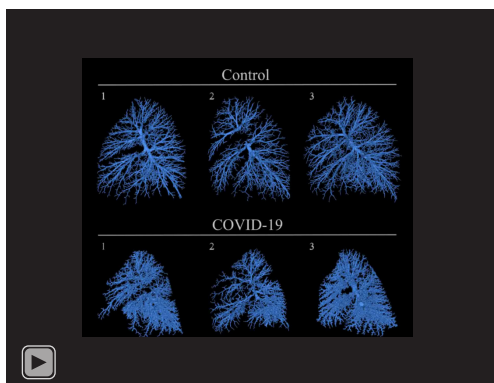
Video 1 Airway segmentations of control compared to COVID-19 lungs (rotating).

present in IPF (*Figure 5*) and likely in other progressive fibrosing lung diseases. Pulmonary embolism and microvascular thrombi are features which are present in COVID-19 patients. Only in COVID-1, the ventilation/perfusion scan was indicative for embolisms but this was not observed on angiogram CT.

Small airway alterations in COVID-19

COVID-19 and IPF lungs were sampled to cover the complete diversity (spectrum) of the pathology (*Figure 6*). Mild disease was characterized by normal alveoli, normal airway/blood vessel architecture with minimal fibrosis
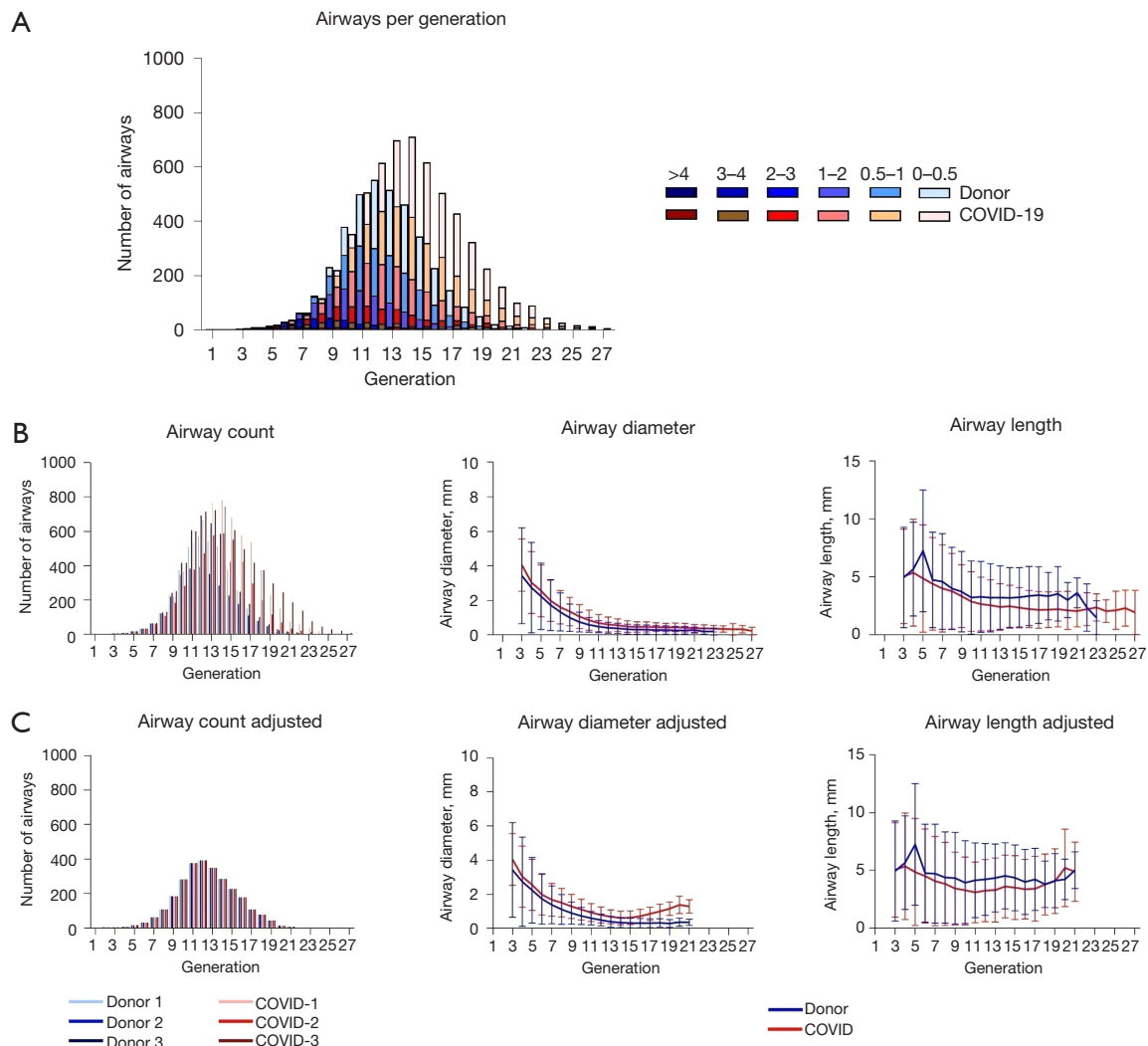
Figure 3 Airway counts are altered in COVID-19. (A) The mean airway numbers are divided in groups according to the diameter for control (blue) and COVID-19 (red) lungs showing more visible airways in COVID-19 lungs with an increase in larger and smaller airways. (B) The number of airways per lung shows more visible airways in COVID-19 (left panel), however, mean diameter (middle panel) and mean length (right panel) did not change. (C) The airway numbers (left panel), mean diameter (middle panel) and mean length (right panel), adjusted to the number of airways per generation of the lung with the fewest visible airways to limit the bias of airway visibility, showed an increase in diameter in the lower generations (generation 17–21). COVID-19, coronavirus disease-19.

starting in the periphery of the secondary pulmonary lobulus. This mild pathology probably develops by increased fibrosis of the periphery of the secondary pulmonary lobulus as seen in IPF (26). More severe distortion started in interstitial spaces of the parenchyma and vessels of the acinus eventually affecting the entire secondary pulmonary lobulus most probably consisting in fibrotic mass as seen in IPF (26). Airway morphology in COVID-19 and IPF lungs was progressively altered in more diseased regions showing

airway enlargement and deformation mainly caused by traction of surrounding fibrotic parenchyma (27). Traction bronchiectasis and bronchodilation are similar to IPF as seen in the airway segmentations (*Figure 6*). However, in IPF, there are more connections between airways and cystic regions, presumably honeycomb cysts which are a hallmark of IPF (27). More airways, likely respiratory bronchioles, were visible due to parenchymal fibrosis and thickening of airway walls, confirming an increase in airway counts.
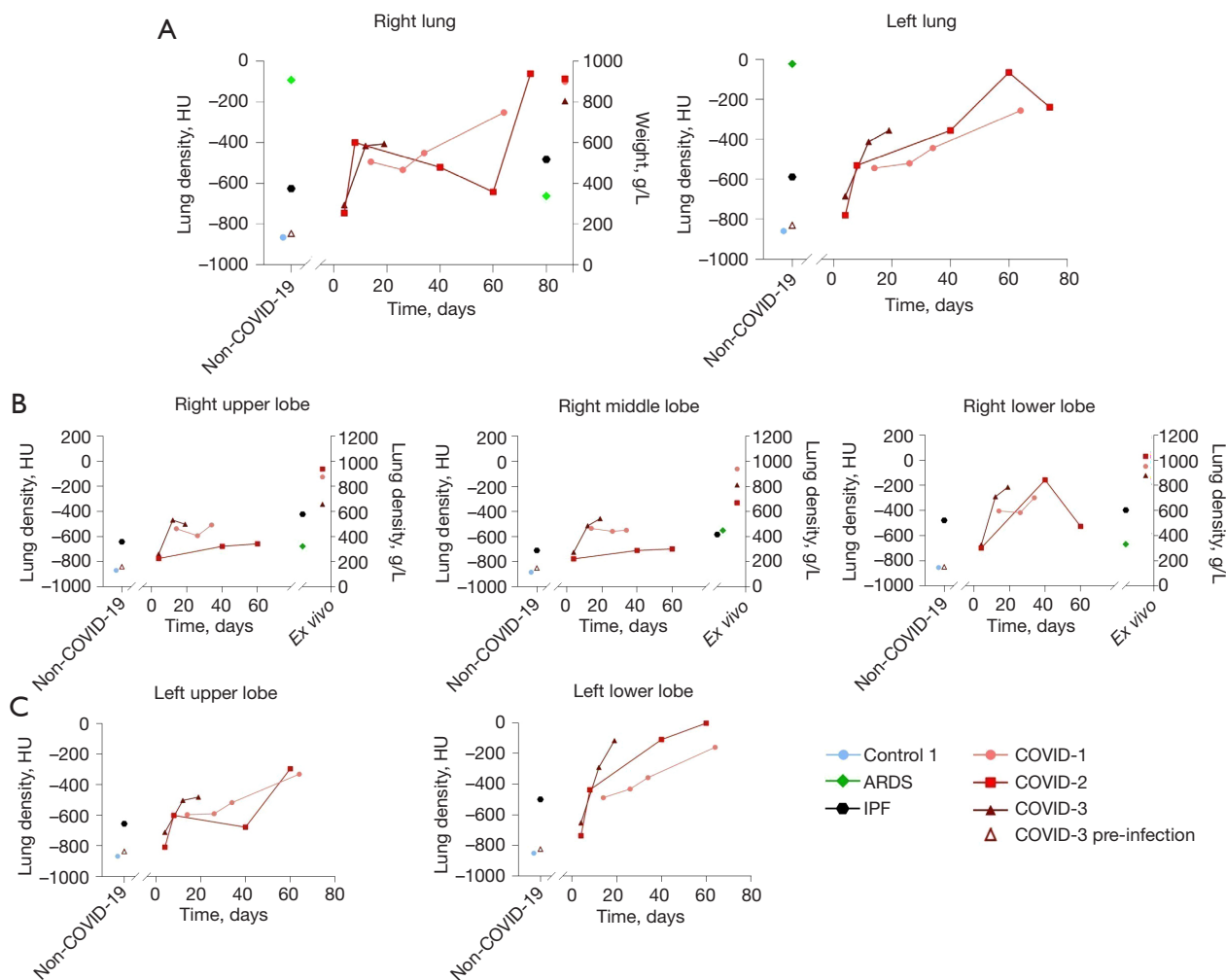
Figure 4 Lung densitometry *in vivo* and *ex vivo*. (A) *In vivo* density increased in the right and left lung already 4 days after onset of symptoms. Density increased gradually over time in the right and left lung, except for COVID-2 showing a transient decline in density of the right lung between day 40 and 60 followed by a dramatical increase. *In vivo* density in IPF and ARDS lungs were also increased compared to non-COVID-19 controls. *Ex vivo* lung density of COVID-19 lungs (g/L) increased and was comparable with *in vivo* density in the last scan (HU). (B) *In vivo* density increased in all lobes but to a greater extent in the lower lobe. For COVID-2, the lower lobe is accountable for the intermediate improvement of the density in the right lung. (C) Density of the left lung lobes increases over time with a higher increase in the lower lobe. Missing values were due to visually unrecognizable fissures. HU, Hounsfield units; COVID-19, coronavirus disease-19; ARDS, acute respiratory distress syndrome; IPF, idiopathic pulmonary fibrosis.

Microthrombi could not be identified using microCT as densities of microthrombi are equal to densities of blood in vessels.

Histological analysis

In all COVID-19 lungs typical characteristics of diffuse alveolar damage (DAD) were present (*Figure 7*). However, different stages of DAD were observed between but also within the same COVID-19 lung. In COVID-1 and 3 an acute stage of DAD with hyalin membranes was observed in the cores indicated as mild on microCT. In the other cores, designated as moderate and severe on microCT, similar patterns were seen in all cores, i.e., an organizing DAD except for COVID-3 which had extensive interstitial fibrosis in the core reported as moderate on microCT. In the most severe core of COVID-3 on microCT, necrotic tissue was present indicating ischemia, however, no (micro)thrombi
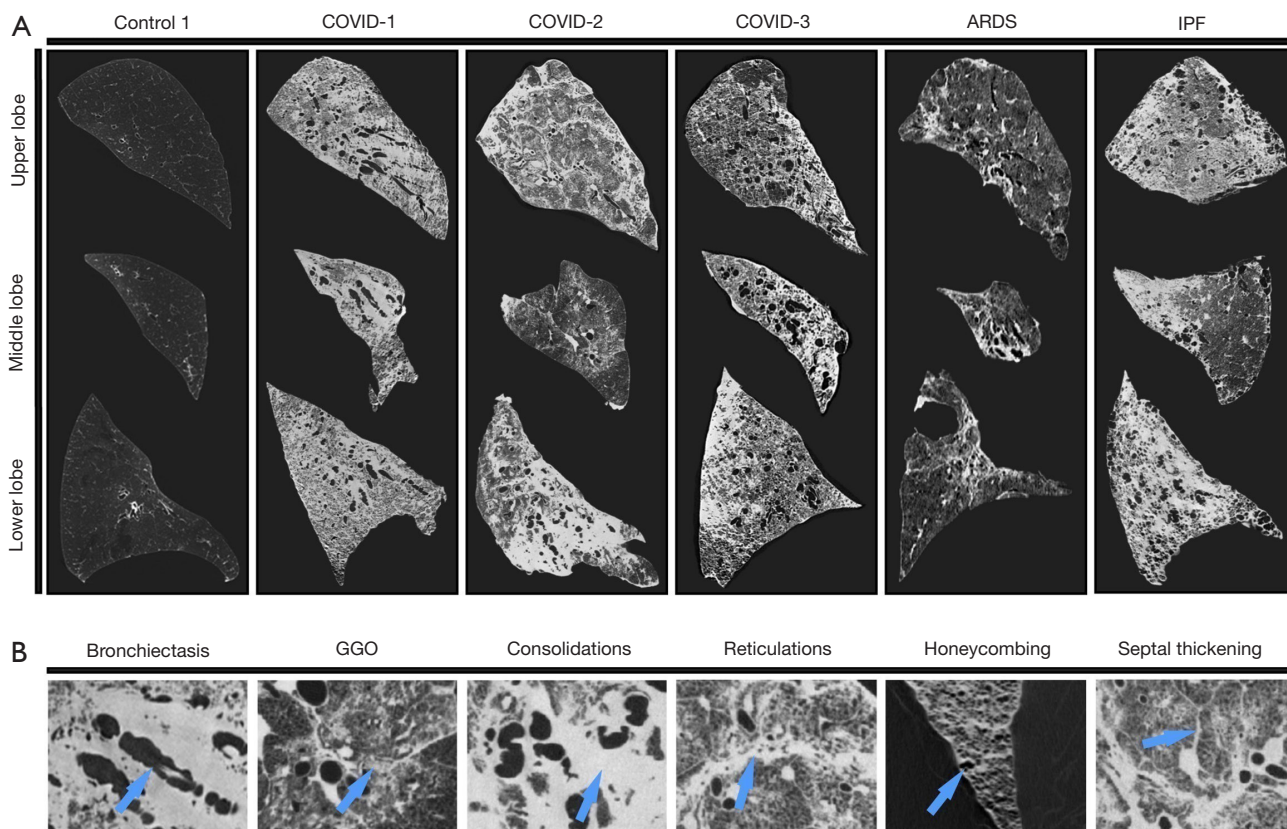
Figure 5 CT features of COVID-19 lungs per lobe compared to control, ARDS, and IPF. (A) Density of COVID-19 lungs is increased in all lobes compared to controls while deterioration is equivalent in ARDS and IPF. (B) The most prevalent and typical CT features (blue arrows) are shown. COVID, coronavirus disease; ARDS, acute respiratory distress syndrome; IPF, idiopathic pulmonary fibrosis; GGO, ground glass opacities; CT, computed tomography.

were found. Organizing pneumonia was present in a limited amount in COVID-2 with intra-alveolar fibroblastic plugs.

Discussion

This study demonstrates the consequences of SARS-CoV-2 induced COVID-19-ARDS on the human lung leading to organized fibrosis in different regions of the lung. The study shows that the lung volume decrease can be followed on serial CT scans with disease progression while density increased, however, different stages of radiological patterns are observed between and within COVID-19 patients. This is also the first study showing small airway pathologies in COVID-19 lungs.

Lung volumes showed an initial rapid decrease with a subsequent gradual decrease over the course of disease, which led to a reduced volume of about 60% in explanted lungs. Similarly, Robbie *et al.* demonstrated that lung volumes decline based on serial CT scans (28). The reduction in lung volume is probably caused by traction of the fibrosis on the periphery of the lung limiting the expansion. Increased lung density as seen in ARDS and IPF, particularly in the lower lobe, was also found in COVID-19 lungs. The rapid onset of disease is in line with previous findings showing rapid abnormal chest CT in hospitalized patients after onset of symptoms (11). Clinically, it is shown that lung volume correlates with pulmonary function tests in IPF, indicating the potential to use this parameter to monitor disease in COVID-19 patients (29).

We showed, for the first time, that the number of visible large and small airways increased in COVID-19, probably caused by thickening of the airway wall and distortion of the lumen as also shown in IPF (30). Large airways were also present in more distal generations in COVID-19 patients as a result of traction bronchiectasis. This will severely impact gas delivery and exchange, leading to aggravation of
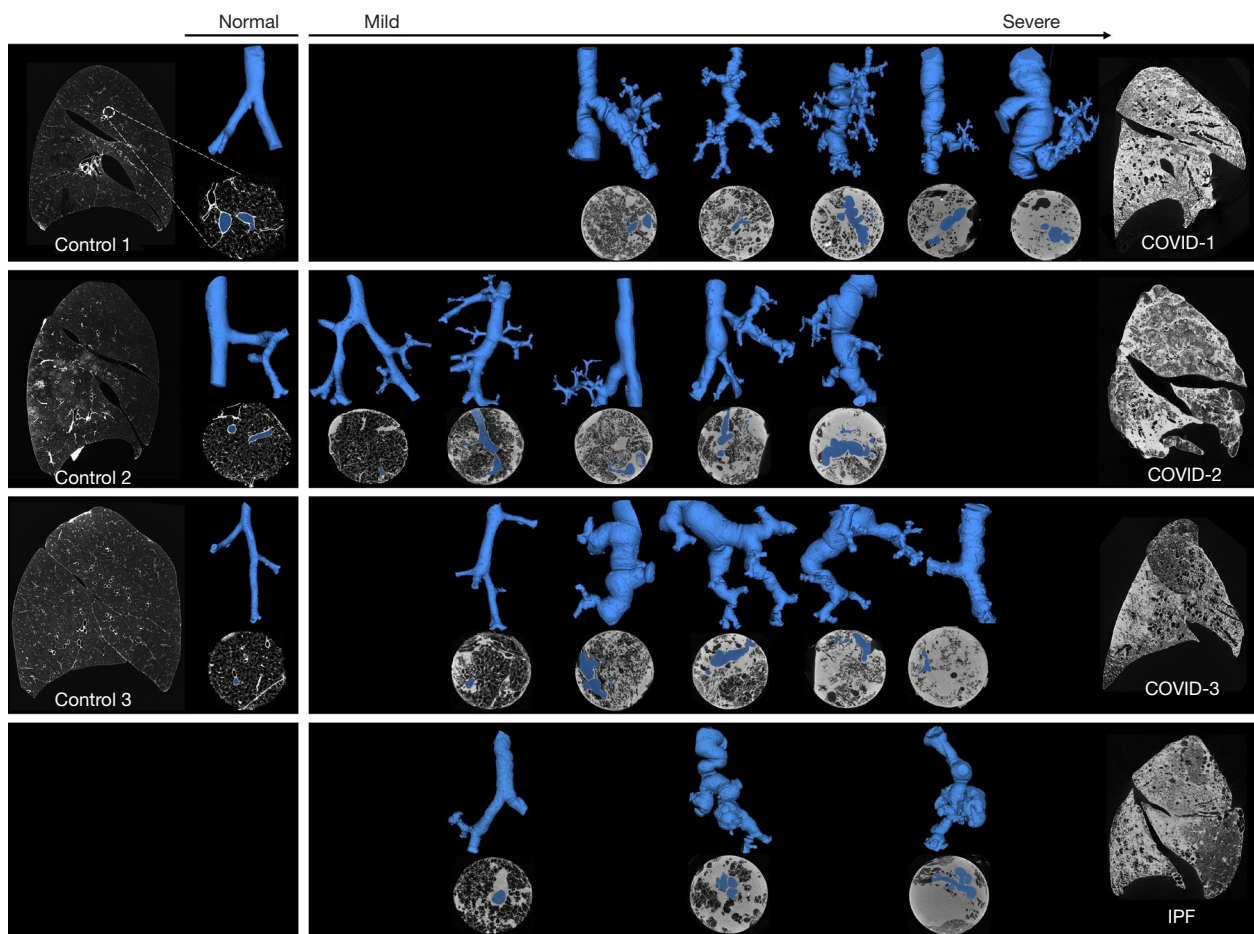
Figure 6 Small airway morphological changes in mild to severe COVID-19 and IPF in comparison to controls. A division was made based on visible characteristics of cores to subdivide the COVID-19 lungs ranging from mild to severe disease. In COVID-19 and IPF, the morphology of the small airways (blue) is severely altered by traction bronchiectasis and the lumen of the airways becomes expanded and varicose. COVID, coronavirus disease; IPF, idiopathic pulmonary fibrosis.

parenchymal changes as pressure and flow will be affected causing alveolar collapse or over expansion.

Density increased in all COVID-19 lungs, however, stages of radiological patterns are different between the transplanted (COVID-1 and 2) patients and the deceased patients (COVID-3). We believe that COVID-1 and 2 are in a further fibroproliferative state affecting whole lobes, while COVID-3 has a more inflammatory ARDS phenotype as depicted by consolidations with beginning fibrosis, however, severe zones of fibrosis are also present in COVID-3 as seen on histology. Consolidations were more present at the anterior and posterior side in the upper and lower lobe respectively (31), most likely caused by gravitational forces (32).

In addition, this study showed microscopic rearrangements in COVID-19 lungs by small-partition microCT consisting in an analogous rearrangement, as seen in IPF, starting in the periphery of the secondary pulmonary lobulus, gradually evolving to the center to become fully fibrotic. Fibrotic rearrangement is irreversible which, in case of COVID-19 evolves much faster compared to IPF. Small-partition microCT also showed that airways were more deformed in severely affected regions.

Histologically, early disease corresponded with microCT findings adding the observations that all patients had DAD. However, in later stages more extensive fibrosis was observed in regions which were categorized as moderate disease on microCT indicating the limitation of discriminating fluids with fibrotic deposition on CT. Nevertheless, this indicates the heterogeneity of COVID-19
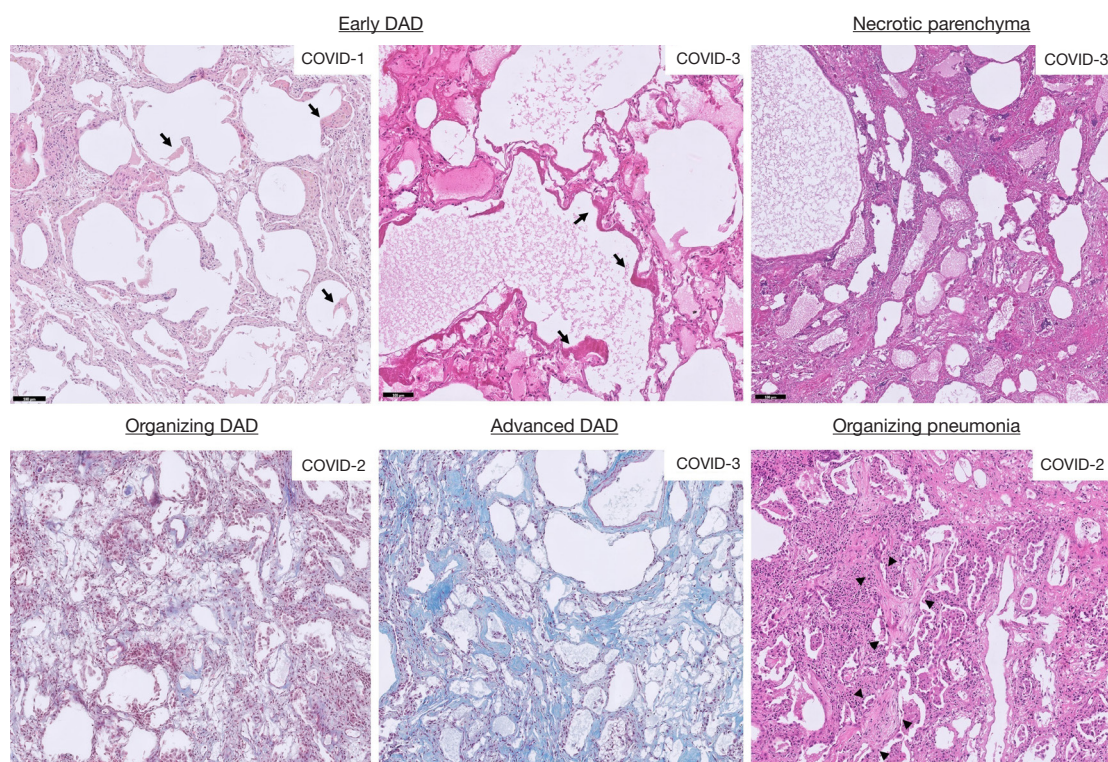
Figure 7 Histological features of COVID-19 lungs. Histology shows different stages of DAD between but also within the same lung. Early stages of DAD were found in COVID-1 and 3 with hyalin membranes (black arrows). A more organizing DAD was observed in all COVID-19 lungs characterized by edema and limited collagen deposition as shown in COVID-2 while in COVID-3, a more advanced organizing stage of DAD was observed on Masson Trichrome staining as abundant collagen fibers were present (blue). Necrotic lung tissue due to ischemia was present in COVID illustrated by the absence of viable cells. In COVID-2, DAD was accompanied by a limited region of organizing pneumonia seen as fibroblastic plugs (black arrowheads). Scale bar =100 µm. DAD, diffuse alveolar damage; COVID, coronavirus disease.

in the lungs. Heterogeneity on pathological sections was also present, however, organizing pneumonia was not observed in the lungs, except in a very confined region of COVID-2, limiting the possibility to discuss the spectrum from organizing pneumonia to DAD. In COVID-3, early and advanced DAD was identified which might explain the rapid deterioration of the patient. Why some patients have no/mild symptoms and other develop COVID-19-ARDS and pulmonary fibrosis is not well known, however, risk factors are described e.g., older age, diabetes, underlying lung diseases etc. (33). We showed many variations between but also within the same lung. This indicates variation in the pathophysiology leading to end-stage disease and implies that radiological, histological, or immunological studies on COVID-19, or other lung diseases, should not be confined to particular regions of the lung. In our cohort, patients were relatively young, but contributing factors such as smoking

for COVID-1 and immunosuppression in the context of a preceding lung transplantation for COVID-3 were present. In addition, during disease course, all patients suffered bacterial or fungal infections probably induced by ventilation (ventilator-associated pneumonia).

This study also suggests that lung volume and density may be used as prognostic factors to identify patients who may potentially benefit from lung transplantation, but further research is needed to investigate the use of volumetric and densitometry to monitor patients as shown in IPF (28,34).

This study has some limitations including the small sample size, due to the fact that COVID-19 patients are not often transplanted, and a lack of in-depth immune typing analysis. In addition, patients were intubated and not able to perform pulmonary function tests or hold their breath during chest CT which might affect density and airway morphology. Yet, we clearly documented how the lung is structurally

destroyed following SARS-CoV-2 infection, resulting in respiratory failure.

Conclusions

In conclusion, this study showed in a very detailed way, using different imaging techniques including microCT, that in some patients, COVID-19 is a rapid aggressive disease destroying the lung architecture including the parenchyma and altering large and small airway morphology. Both will contribute to disease progression, eventually leading to the need for transplantation or death. This paper indicates that clinicians should continue using follow-up CT to monitor severely affected patients.

Footnote

Reporting Checklist: The authors have completed the STROBE reporting checklist. Available at https://jtd.amegroups.com/article/view/10.21037/jtd-22-1488/rc

Data Sharing Statement: Available at https://jtd.amegroups.com/article/view/10.21037/jtd-22-1488/dss

Conflicts of Interest: Conflicts of Interest: All authors have completed the ICMJE uniform disclosure form (available at https://jtd.amegroups.com/article/view/10.21037/jtd-22-1488/coif). BMV, GGR, WAW, and WJ report funding from KU Leuven (No. C16/19/005). WAW reports funding from Roche, Boehringer Ingelheim, and Galapagos. GMV and DEVR report funding from the Broere Charitable Foundation. LJC reports funding from Medtronic. RV reports funding from UZ Leuven (No. STG15/023). RV, VG, JK, A Vanstapel, TG, MV, and IG report funding from the Research Foundation-Flanders (FWO) (No. 12G8715N to RV, No. 11L9822N to VG, No. 1198920N to JK, No. 1102020N to A Vanstapel, No. 1S73921N to TG, No. 1SE4322N to MV, and No. 11N3922N to IG). MNB reports funding from the Ghent University Special Research Fund for the UGCT Centre of Expertise BOF. EXP.2017.0007. The other authors have no conflicts of interest to declare.

Ethical Statement: The authors are accountable for all aspects of the work in ensuring that questions related to the accuracy or integrity of any part of the work are appropriately investigated and resolved. The study was conducted in accordance with the Declaration of Helsinki (as revised in 2013). The study was approved by the Ethical Committee of UZ/KU Leuven (Nos. S51577 and S52174). Written informed consent was obtained from patients for the use of samples for research. Discarded donor lungs were collected in accordance with Belgian law stating that all qualified donors of which organs are not of sufficient quality or remain unused for other reasons can be used for research.

References

1. WHO Coronavirus (COVID-19) Dashboard. WHO Coronavirus (COVID-19) Dashboard With Vaccination Data. Available online: https://covid19.who.int/
2. Wiersinga WJ, Rhodes A, Cheng AC, et al. Pathophysiology, Transmission, Diagnosis, and Treatment of Coronavirus Disease 2019 (COVID-19): A Review.

JAMA 2020;324:782-93.

3. Jafari-Oori M, Ghasemifard F, Ebadi A, et al. Acute Respiratory Distress Syndrome and COVID-19: A Scoping Review and Meta-analysis. Adv Exp Med Biol 2021;1321:211-28.

4. Ferguson ND, Fan E, Camporota L, et al. The Berlin definition of ARDS: an expanded rationale, justification, and supplementary material. Intensive Care Med 2012;38:1573-82.

5. Batah SS, Fabro AT. Pulmonary pathology of ARDS in COVID-19: A pathological review for clinicians. Respir Med 2021;176:106239.

6. Huang C, Huang L, Wang Y, et al. 6-month consequences of COVID-19 in patients discharged from hospital: a cohort study. Lancet 2021;397:220-32.

7. Montani D, Savale L, Noel N, et al. Post-acute COVID-19 syndrome. Eur Respir Rev 2022;31:210185.

8. Long Q, Li J, Hu X, et al. Follow-Ups on Persistent Symptoms and Pulmonary Function Among Post-Acute COVID-19 Patients: A Systematic Review and Meta-Analysis. Front Med (Lausanne) 2021;8:702635.

9. Fang Y, Zhang H, Xie J, et al. Sensitivity of Chest CT for COVID-19: Comparison to RT-PCR. Radiology 2020;296:E115-7.

10. Ai T, Yang Z, Hou H, et al. Correlation of Chest CT and RT-PCR Testing for Coronavirus Disease 2019 (COVID-19) in China: A Report of 1014 Cases. Radiology 2020;296:E32-40.

11. Wang Y, Dong C, Hu Y, et al. Temporal Changes of CT Findings in 90 Patients with COVID-19 Pneumonia: A Longitudinal Study. Radiology 2020;296:E55-64.

12. Liu N, He G, Yang X, et al. Dynamic changes of Chest CT follow-up in Coronavirus Disease-19 (COVID-19) pneumonia: relationship to clinical typing. BMC Med Imaging 2020;20:92.

13. Watanabe A, So M, Iwagami M, et al. One-year follow-up CT findings in COVID-19 patients: A systematic review and meta-analysis. Respirology 2022;27:605-16.

14. Simpson S, Kay FU, Abbara S, et al. Radiological Society of North America Expert Consensus Document on Reporting Chest CT Findings Related to COVID-19: Endorsed by the Society of Thoracic Radiology, the American College of Radiology, and RSNA. Radiol Cardiothorac Imaging 2020;2:e200152.

15. Kwee RM, Adams HJA, Kwee TC. Diagnostic Performance of CO-RADS and the RSNA Classification System in Evaluating COVID-19 at Chest CT: A Meta-Analysis. Radiol Cardiothorac Imaging 2021;3:e200510.

16. Adams HJA, Kwee TC, Yakar D, et al. Chest CT Imaging Signature of Coronavirus Disease 2019 Infection: In Pursuit of the Scientific Evidence. Chest 2020;158:1885-95.

17. Goyal N, Chung M, Bernheim A, et al. Computed Tomography Features of Coronavirus Disease 2019 (COVID-19): A Review for Radiologists. J Thorac Imaging 2020;35:211-8.

18. Machnicki S, Patel D, Singh A, et al. The Usefulness of Chest CT Imaging in Patients With Suspected or Diagnosed COVID-19: A Review of Literature. Chest 2021;160:652-70.

19. Zhao W, Zhong Z, Xie X, et al. Relation Between Chest CT Findings and Clinical Conditions of Coronavirus Disease (COVID-19) Pneumonia: A Multicenter Study. AJR Am J Roentgenol 2020;214:1072-7.

20. Shi F, Wei Y, Xia L, et al. Lung volume reduction and infection localization revealed in Big data CT imaging of COVID-19. Int J Infect Dis 2021;102:316-8.

21. Sava R, Öz Özcan A. Evaluation of lung volume loss with 3D CT volumetry in COVID-19 patients. Diagn Interv Radiol 2021;27:155-6.

22. Verleden SE, Kirby M, Everaerts S, et al. Small airway loss in the physiologically ageing lung: a cross-sectional study in unused donor lungs. Lancet Respir Med 2021;9:167-74.

23. Coxson HO. Lung parenchyma density and airwall thickness in airway diseases. Breathe 2012;9:36-45.

24. Yushkevich PA, Piven J, Hazlett HC, et al. User-guided 3D active contour segmentation of anatomical structures: significantly improved efficiency and reliability. Neuroimage 2006;31:1116-28.

25. McDonough JE, Yuan R, Suzuki M, et al. Small-airway obstruction and emphysema in chronic obstructive pulmonary disease. N Engl J Med 2011;365:1567-75.

26. Mai C, Verleden SE, McDonough JE, et al. Thin-Section CT Features of Idiopathic Pulmonary Fibrosis Correlated with Micro-CT and Histologic Analysis. Radiology 2017;283:252-63.

27. Hansell DM, Bankier AA, MacMahon H, et al. Fleischner Society: glossary of terms for thoracic imaging. Radiology 2008;246:697-722.

28. Robbie H, Wells AU, Fang C, et al. Serial decline in lung volume parameters on computed tomography (CT) predicts outcome in idiopathic pulmonary fibrosis (IPF). Eur Radiol 2022;32:2650-60.

29. Robbie H, Wells AU, Jacob J, et al. Visual and Automated CT Measurements of Lung Volume Loss in Idiopathic Pulmonary Fibrosis. AJR Am J Roentgenol

2019;213:318-24.

30. Verleden SE, Tanabe N, McDonough JE, et al. Small airways pathology in idiopathic pulmonary fibrosis: a retrospective cohort study. Lancet Respir Med 2020;8:573-84.

31. Zompatori M, Ciccarese F, Fasano L. Overview of current lung imaging in acute respiratory distress syndrome. Eur Respir Rev 2014;23:519-30.

32. Khullar R, Shah S, Singh G, et al. Effects of Prone Ventilation on Oxygenation, Inflammation, and Lung Infiltrates in COVID-19 Related Acute Respiratory Distress Syndrome: A Retrospective Cohort Study. J Clin Med 2020;9:4129.

33. Ejaz H, Alsrhani A, Zafar A, et al. COVID-19 and comorbidities: Deleterious impact on infected patients. J Infect Public Health 2020;13:1833-9.

34. Loeh B, Brylski LT, von der Beck D, et al. Lung CT Densitometry in Idiopathic Pulmonary Fibrosis for the Prediction of Natural Course, Severity, and Mortality. Chest 2019;155:972-81.